Available Online http://www.ijncse.com
ISSN Online: 2395-7018

# INTERNATIONAL JOURNAL OF NANO CORROSION SCIENCE AND ENGINEERING

Impact Factor: 4.980

Volume 4 , Issue 1, March , 2017

Prof Dr S Rajendran

Editor-in-Chief

Available Online http://www.ijncse.com
ISSN Online: 2395-7018
INTERNATIONAL JOURNAL OF NANO CORROSION SCIENCE AND ENGINEERING

# MICRO- AND NANO-ELECTROCHEMICAL INVESTIGATIONS OF COPPER CORROSION AND ITS INHIBITION WITH SELECTED ORGANIC MOLECULES

***Abdul Shaban[1*], Gyöngyi Vastag[2] and Ilona Felhősi***

[1]Functional Interfaces Group, Institute of Materials and Environmental Chemistry, Research Centre for Natural Sciences, H. A. S., 1117 Budapest, Magyar tudósok körútja 2.

[2]University of Novi Sad, Faculty of Sciences, Department of Chemistry, Biochemistry and Environmental Protection, Trg Dositeja Obradovića 3, 21000 Novi Sad, Serbia.

*Corresponding author. E-mail: shaban.abdul@ttk.mta.hu

## Abstract

The objective of this investigation was to gain information concerning the processes involved in the corrosion of copper and its inhibition in acidic 0.1 mol. $dm^{-3}$ $Na_2SO_4$ solutions. Thiazole derivatives containing functional groups were chosen for this investigation. The electrochemical behavior of copper and the inhibitor efficiency of the thiazole derivatives against copper corrosion were followed by electrochemical impedance spectroscopy (EIS) and the electrochemical quartz microbalance (EQCM). It was found that the anticorrosion protection provided by these thiazoles followed the sequence: 5-IPBDT > 5-BDT > 5-TDT > 5-MBDT. The thickness of the adsorbed layers did not grow as time elapsed, and amounted to a mono or partial monolayer. Scanning electrochemical microscopy (SECM) was employed to investigate the occurrence of conductivity changes at the surface of the copper specimens when exposed to an inhibitor containing solution. The results showed that adsorption of the inhibitors did not produce any changes in the conductivity of the surface films. Nanoscopic changes on the metal surface were monitored in situ with atomic force

(AFM) and scanning tunneling (STM) microscopes. AFM images showed that surface smoothing occurred in the presence of the inhibitors. Surface reorganization at the atomic level was evidenced by EC-STM.

**Keywords:** thiazole derivatives; EIS; polarization measurements; AFM; QCM;

## 1. Introduction

Most metallic materials are used in a state of passivity in which the corrosion rate is very low due to an intervening oxide film caused by reaction of the metal with the environment. The passive film provides a powerful barrier towards ionic migration, thus retarding the rate at which metal ions enter the solution phase. However, localised de-passivation can take place when this passive state is broken down under the influence of aggressive ions from the environment. During localised corrosion, most of the metal surface remains inactive, while in isolated areas, the development of corrosion pits leads to failures by perforation of the material.

Copper is a metal with a low redox potential in aqueous solutions [1], and it constitutes a representative example for the study of the electrochemical behaviour of passive materials. Copper is extensively used in various industrial applications due to its interesting properties, namely high electrical and thermal conductivities. Moreover, it exhibits a high corrosion resistance due to the formation at its surface of a uniform and adherent oxide film by the corrosion process itself. This passive film protects copper from the aggressive medium.

The electrochemistry of copper in alkaline aqueous solutions has been extensively studied in relation to the protective characteristics of passive films [2-19]. The onset of passivity has been related to the formation of copper oxide layers with a duplex structure, consisting in general terms of an inner $Cu/Cu_2O$ porous and an outer CuO hydrated layers [7, 8]. The properties of the passive layer such as thickness, structure and protection effectiveness depend on the solution composition, the copper surface treatment, the temperature and the potential routine employed in the experiments [5-8, 11-19].

However, in spite of this self-protecting property, copper is susceptible to corrosion by acids and strong alkaline solutions, especially in the presence of oxygen or oxidants. In the pH range between 2 and 5, the dissolution of Cu is very rapid, and the formation of a stable

surface oxide layer, which would passivate the metal surface, is hindered. An oxide surface layer can only be formed in weak acid or alkaline solutions. Several reaction schemes have been proposed in the scientific literature in an attempt to explain the dissolution processes of copper in acidic media [20–24].

One of the most important methods for the protection of metals is the use of organic inhibitors to protect the metal surface from the corrosive environment. The effectiveness of organic inhibitors is related to the extent to which they adsorb and cover the metal oxide surface. In the case of adsorption-type inhibitors, the anticorrosive protection can be explained by the Lewis acid-base interaction on metal surfaces. The major factors that influence this interaction are the molecular structure of the compounds [20], the surface charge on the metal, and the type of the electrolyte [25]. Heterocyclic organic compounds containing nitrogen, sulphur or oxygen atoms are often used to protect metals from corrosion due to the ability of the heterocyclic atoms to easily form bonds with transition metals such as copper [20, 21, 26–34]. Thus, several inhibitors like azoles, triazoles, and sulfoxide derivatives have been known and successfully been applied for the protection of copper [35-40], and some investigators have proposed that the inhibition effectiveness might be due to the formation of thin layers of copper-inhibitor complexes [41, 42]. Azoles such as 2-mercaptobenzimidazole, benzotriazole, and tolyltriazole are extensively used for such applications [7, 43-46]. These inhibitors are very effective in alkaline and neutral environments, but less effective in acidic solutions [47–49]. So far, benzotriazole is probably the most efficient substance for the inhibition of copper corrosion in those environmental conditions, and it has become the most commonly used in practice.

However, owing to stricter environmental regulations, low inhibitor toxicity is an important requirement in the choice of inhibitors to be employed. Thus, the latest trend in industry is to replace toxic inhibitors, such as triazoles, with nontoxic organic chemicals that cause no harm to the environment. In closed systems, thiazole derivatives have been found to be an excellent replacement for the toxic triazoles, and some thiazoles derivatives have already presented excellent inhibition properties.

In the past few decades the study of the action mechanism of inhibitors was performed using conventional electrochemical methods [50-52], but in recent times a growing number of

research groups have started to employ in situ surface sensitive techniques in order to better understand the processes that take place on the metal surfaces. Two groups of techniques have become increasingly used in this area, namely scanning probe microscopies (SPM), and the electrochemical quartz crystal microbalance (EQCM). SPM methods have been employed to investigate the electrodissolution of copper in acidic environments containing benzotriazole, and the occurring surface morphological changes were imaged in micro-meter and nano-meter scales [53-58]. On the other hand, the EQCM has been successfully employed to determine the efficiencies of several corrosion inhibitors due to its ability to measure mass differences in the order of nanograms per surface area [30-34, 59, 60]. Even more recently, a new approach to these studies has been opened by Kontturi and co-workers by using the scanning electrochemical microscope (SECM) to investigate the mechanism of copper corrosion inhibition by benzotriazole in moderately alkaline electrolytes [61, 62].

In this study of the effectiveness of several potential copper corrosion inhibitors in acidic media was examined. The purpose was to gain in situ information about of the corrosion and inhibition processes of copper in acidic environment by thiazole derivative functional groups containing heterocyclic atoms such as nitrogen, sulphur, and oxygen. Several techniques have been employed to get complementary information on the electrochemical and the surface reactions, namely EIS, QCM, SECM, STM, and AFM.

notations. The violin is called blind instrument, because there is no fixed notes (notation). The description of violin is shown in figure 2.

## 2. Methodology

Copper materials used in this study were available in three different forms, namely: polycrystalline Cu was used for the electrochemical, SECM and AFM studies; Cu (111) single-crystal was employed for EC-STM experiments; and electrochemically deposited copper layers were used for QCM measurements.

Polycrystalline copper was supplied as a sheet of thickness 1 mm (99.99%) which was cut into square specimens of area ca. 1 $cm^2$. The surface of the copper specimen was polished both mechanically and electrically. Mechanical polishing was done first with silicon carbide papers of 800 and 4000 grit and with aluminium micro-polish (0.3 mm particle size). Then

the sample was rinsed with water and ethanol and electropolished at 3 V for ca. 2 min in a solution of concentrated phosphoric and sulphuric acids (77% $H_3PO_4$, 11.5% $H_2SO_4$, and 11.5% $H_2O$ by volume). The copper substrate was used as the anode and a copper sheet was used as the cathode. After electropolishing the copper substrate was cleaned in an ultrasonic bath in milli-Q water for 10-15 min and twice in ethanol for 20 min.

Cu(111) single crystals were first polished mechanically (down to 0.25 μm diamond paste) and then electrochemically polished, in 66% ortho-phosphoric acid, for 10 min, at an anodic potential value of 1.8 V vs. a Cu counter electrode. After etching, the crystals were thoroughly rinsed with Milli-Q water. Copper layers were galvanostatically electrodeposited on one face of the gold-covered quartz crystal. Copper was deposited from an acidic copper bath consisting of 0.5 M $CuSO_4$, 0.5 M $H_2SO_4$, and 1 M $C_2H_5OH$ solution.

The following thiazole-derivative inhibitors were considered in this work: 5-benzylidene-2,4-dioxotetrahydro-1,3-thiazole (5-BDT), 5-(4′-isopropylbenzylidene)-2,4-dioxotetrahydro-1,3-thiazole (5-IPBDT), 5-(3′-thenylidene)-2,4-dioxotetrahydro-1,3-thiazole (5-TDT), 5-(3′,4′-dimetoxybenzylidene)-2,4-dioxotetrahydro-1,3-thiazole (5-MBDT). The concentration of the inhibitors in the base solution was in the order of $10^{-5}$ M. The electrolyte solution was 0.1 M $Na_2SO_4$ at pH of 2.94. All experiments were performed at open atmosphere and room temperature.

### *2.1 QCM measurements*

The quartz crystal used was an AT-cut disk of 12 mm diameter and of 10-MHz nominal oscillation frequency. Frequency changes, which were converted to mass changes, of the quartz electrode, were registered in time at the open circuit potential. A calibration plot of frequency change versus time was constructed during copper electrodeposition as can be seen in fig. 1. Using Sauerbrey's equation [63], frequency change is related to mass change which is calculated from Faraday's law, thus producing the quartz crystal sensitivity constant ($C_f$). Since nearly no current loss occurs under the deposition conditions, the amount of deposited metal *($\Delta m$)* is:

$$\Delta m = \frac{M_W \, i \, n \, \Delta t}{2F} \qquad (1)$$

where i is the current density applied; MW, is the copper atomic weight; n, is the number of electrons involved, and F is Faraday's constant.

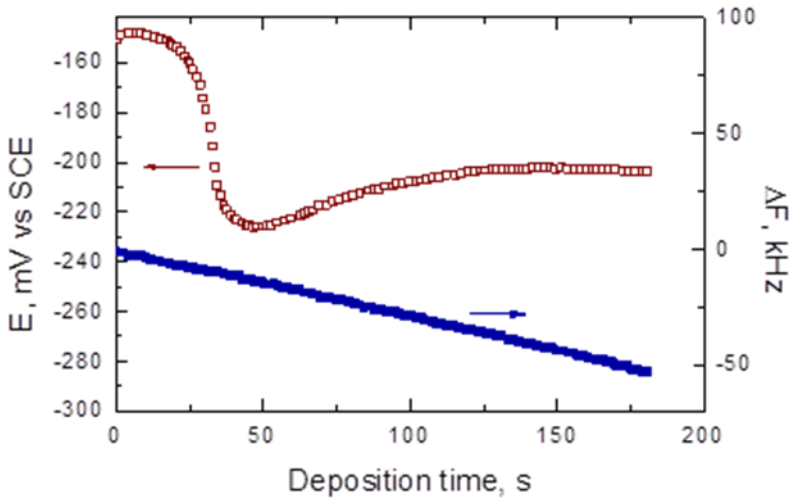


**Figure 1: Calibration curve of frequency change, due to copper electrodeposition, and potential change versus time, to determine quartz crystal sensitivity coefficient**

During acidic media experiments, the mass change due to dissolution could be expressed as thickness reduction rate, which is more practical for estimating the corrosion damage:

$$\delta = \frac{\Delta m}{A \rho t} \tag{2}$$

where δ, is the thickness reduction rate; ρ, is the copper density; A, is the electrode active area, and Δm, is the mass loss.

***2.2 EIS measurements***

EIS experiments were carried out in a three-electrode cell constituted of the polycrystalline copper-working electrode, saturated calomel as reference electrode and a Pt wire as counter electrode. Data were collected at the corrosion potential in a frequency range between 0.01 and 10,000 Hz.

***2.3 SECM measurements***

The measurements were carried out in a three-electrode cell with an Ag/AgCl/KCl saturated reference electrode and a Pt counter electrode. The reference electrode was connected to the cell using a salt bridge to avoid chloride ion contamination. The SECM tip (working

electrode) used in the measurements consisted of a Pt wire with a diameter of 10 µm sealed in a glass capillary. The experiments were carried out under normal atmosphere using a CHI-900 scanning electrochemical microscope. The tip was characterized using ferrocene-methanol solution as electrochemical mediator. The measurements were performed both in the absence and in the presence of the inhibitors. The measurement sequence consisted of the following steps:

1. the copper substrate, immersed in a solution of 1 mM ferrocene-methanol + 0.1 M Na2SO4, was held at - 0.40 V during 10 minutes,
2. then the substrate was held at -1.05 V during 6 minutes to reduce any residual copper oxide left on the surface, and,
3. immediately after the reduction step, the solution was changed to a clean solution, whereas the substrate was left unpolarised.

### *2.4 SPM experimental details*

In situ STM was used to study processes at solid/liquid interface at nanoscale. Local investigations of copper single-crystal electrode surfaces have been studied in electrochemical environment using a PicoStat instrument. The tunnelling tips were made of Pt and covered with an epoxy layer up to the operational tip, to decrease the faradaic current [64].

Morphological changes on the electrode surface were also monitored by atomic force microscopy (AFM) with a Nanoscope III apparatus.

## 3. Results and Discusion

### *3.1 Gravimetric tests*

The influence of the selected thiazoles on copper corrosion was investigated by monitoring the mass changes of the copper electrode using QCM. The experiments consisted in a sequence of three steps proposed by Kálmán and co-workers [23, 31]. In the first interval a blank solution was introduced in the measurement cell, namely acidic 0.1 M $Na_2SO_4$ test solution. In the second interval the electrolyte was exchanged with an inhibitor-containing electrolyte for a longer exposure period, while in the third interval the blank solution was applied again. The experiments were conducted until most of the deposited copper was

removed or there was no significant change of the electrode frequency. The gravimetric plots measured with this experimental procedure are given in fig. 2.

The electrode mass decreased with time for copper specimens immersed in acidic 0.1 M $Na_2SO_4$ solution at all times, which indicated that the copper dissolution proceeded due to corrosion process. During the first interval, all experiments showed practically the same behavior, and minor differences can be related to differences in surface roughness of the copper electrodes originated during the electrodeposition process.

The addition of 5-IPDBT and 5-BDT inhibitors showed significant decreases in the electrode mass change during the second interval. The presence of these thiazole derivatives slowed the Cu dissolution, and the electrode mass change almost stabilized during this period. However, 5-TDT and 5-MBDT inhibitors did not produce as much protection, and in spite of their presence in the electrolyte, the copper sample continued to dissolve at rather high rates.

In the third interval, the absence of the inhibitor resulted in a increase of the corrosion rate, though not as high as it was in the first step. This fact is an indication that some adsorbed inhibitor molecules or complexes remained on the electrode surface after electrolyte exchange.

The behavior of the inhibitors showed no increase of the electrode mass due to the adsorption of the inhibitor, which is indicative that those inhibitors adsorbed as a two dimensional type. The thickness of these layers did not grow in size and were in the order of a mono or even partial monolayer.

By using Faraday's law, the Cu thickness reduction rate was calculated and results are listed in Table 1. Table 1 shows that the highest inhibitor efficiency (90%) was provided by the applications of 5-IPBDT. These results could be predicted because 5-IPBDT is a larger molecule due to its longer chain.

### *3.2 EIS results*

The EIS measurements provided information about of the electrochemical behavior of the copper during the exposure at 0.1 M Na2SO4 acidified solution and the effect of the thiazole derivatives inhibitors addition. The effectiveness differences between the tested inhibitors in

this work were obtained in terms of polarization resistances which were determined from the impedance spectra, given in figs. 3 and 4.

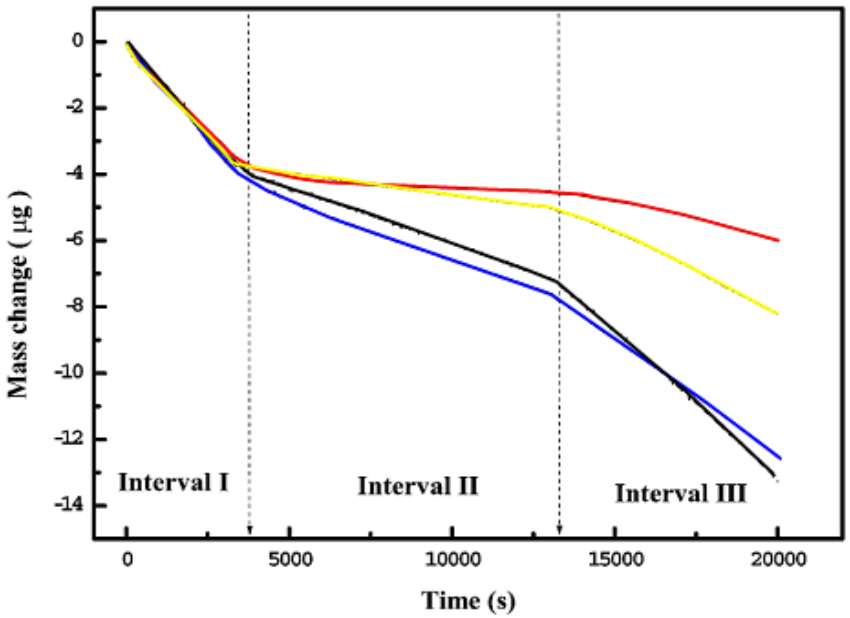


**Figure 2: Time dependence of mass changes of Cu in acidic 0.1 M Na2SO4 solution without and with the thiazole derivatives:**
**(—) 5-IPBDT, (—) 5-BDT, (—) 5-TDT, and (—) 5-MBDT.**

| Solutions | Thickness reduction rate, µm year$^{-1}$ | η % |
|---|---|---|
| Blank | 126 | - |
| 5-IPBDT | 15 | 89 |
| 5-BDT | 18 | 86 |
| 5-TDT | 44 | 65 |
| 5-MBDT | 47 | 73 |

**Table 1. Thickness reduction rate of copper in $Na_2SO_4$ (pH 2.9) with the addition of thiazole derivatives**

Figure 3 shows the comparison of the Nyquist plots obtained for the copper immersed in electrolyte solution without and with the studied inhibitors. From the observation of the plots

was clearly deduced that the 5-IPBDT inhibitor presented the highest impedance values. This behavior was an indication of the formation of an effective protective film that hindered corrosion of the metal after the 5-IPBDT addition.

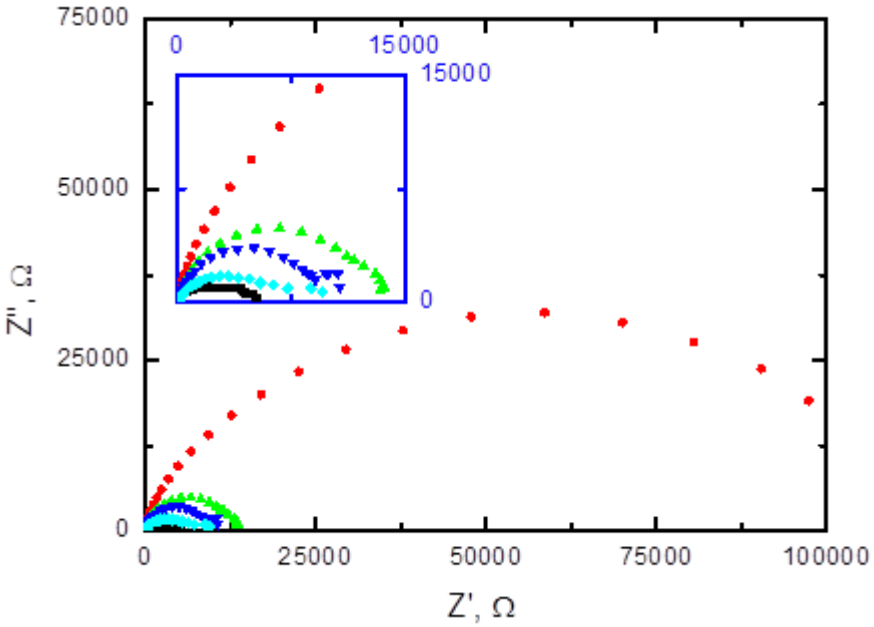


**Figure 3. Nyquist plots of copper electrode immersed in 0.1 M $Na_2SO_4$ solution (—) in the absence of inhibitor, and in the presence of (—) 5-MBDT, (—) 5-TDT, (—) 5-BDT or (—) 5-IPBDT inhibitors. The concentration of the inhibitor solutions was $10^{-5}$ M.**

This fact was confirmed from the values of the polarization resistance, Rp showed in the Table 2. The Rp values were determinate by calculating the semicircle intersection with the real part of the impedance amplitude. The inhibition efficiency (η%) was determined using:

$$\eta(\%) = \left(1 - R_p^{inh} / R_p^0\right) \cdot 100 \quad (3)$$

where and represent the electrode polarization resistance in the absence and presence of the inhibitor in the electrolyte, respectively.

Figure 4 shows the Bode plots for the tested thiazole derivatives. Phase shift vs. the logarithm of the frequency gave an indication of the behavior of the protective film formed on the electrode surface due to the inhibitor adsorption. It can be seen from this figure that the process taking place at the electrode surface has one relaxation time constant. The location of the relaxation time constant did not change much from one inhibitor, but the phase shift value

increased with 5-IPBDT having the highest value at the peak location. This is an indication that the adsorption of all inhibitors on the electrode surface follows the same pattern but with different intensities.

| Inhibitor | 5-IPBDT | 5-BDT | 5-TDT | 5-MBDT |
|---|---|---|---|---|
| $R_p$, kΩ | 115 | 15 | 9.3 | 7.3 |
| Inhibitor efficiency, % | 93 | 86 | 80 | 71 |

**Table 3: EIS results for the tested thiazole derivatives.**

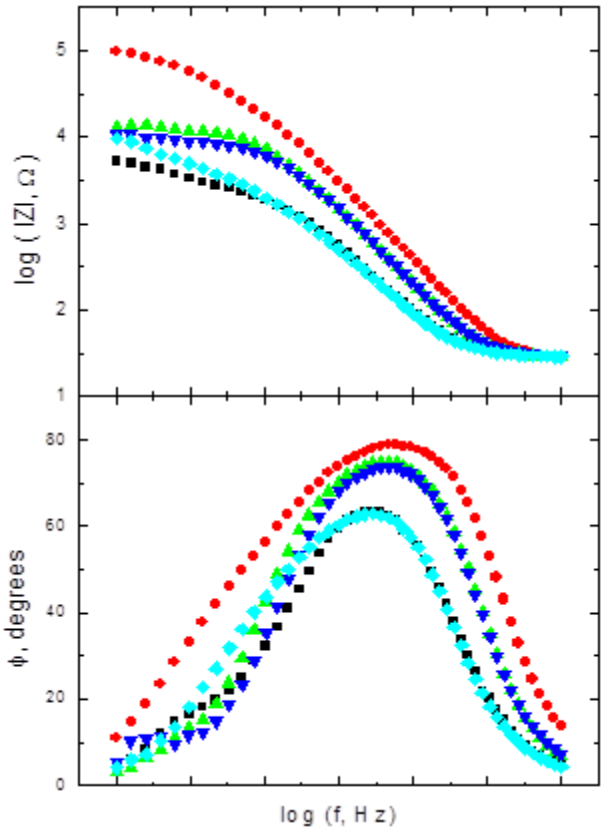


**Figure 4. Bode plots of copper electrode immersed in 0.1 M $Na_2SO_4$ solution (—) in the absence of inhibitor, and in the presence of (—) 5-MBDT, (—) 5-TDT, (—) 5-BDT or (—) 5-IPBDT inhibitors. The concentration of the inhibitor solutions was $10^{-5}$ M.**

In summary, EIS measurements have shown that the order of protection efficiency provided by the thiazole inhibitors was as follows: 5-IPBDT > 5-BDT > 5-TDT > 5-MBDT. This could be explained by the presence of N and S in the molecule structure, and the longer chain served as a protecting shield on the copper electrode surface.

***3.3 SECM results***

SECM was employed to monitor whether the activity of the inhibitors present in the solution phase might induce variations in the conductivity of the copper surface. Imaging of the surface was also accomplished with the SECM at selected time intervals. The duration of the experiments was 3 hours for each system.

The study was carried out by measuring the approach curves of the SECM tip towards the sample surface, for what ferrocene-methanol was used as the electrochemical mediator, and the tip potential was set at + 0.5 V vs. Ag/AgCl/KCl saturated reference electrode.

The experimental procedure consisted in a series of steps as described next. The approach curve was measured first in the test solution in the absence of the inhibitor. Then, without shifting the position of the tip in the horizontal plane, the solution was changed to the inhibitor-containing solution, and approach curves were measured at different exposure times. With this procedure the approach curves were measured on the same spot of the surface, both in presence and absence of the protective species, and therefore, effects of surface roughness of the substrate could be minimized.

Figure 5 shows the sequence of approach curves obtained on copper samples exposed to the various thiazole derivatives under investigation. The typical response of a conducting substrate was found in all cases, that is, the current measured at the SECM-tip increased as the substrate was approached (i.e., positive feedback regime). For a given inhibitor, the curves measured at different exposure times could be superimposed, thus confirming that the conductivity of the surfaces did not vary during the corrosion process. Indeed, the topography of the samples did not significantly changed during the experiments, and the images showed a rather featureless surface in all cases (fig. 6). Therefore, the scanning electrochemical microscope confirms that no localized effects were observed at a micrometer scale during copper electrodissolution in the acidic 0.1 M $Na_2SO_4$ solution. That is, metal corrosion takes place homogeneously in this environment both in the absence and in the presence of the

inhibitors. These results are in agreement with the electrochemical evidences that the inhibitors do not form 3D layers on the surface of the metal in these conditions.

### *3.4 AFM and STM imaging*

The application of SPM techniques was used to follow the nanoscopic changes of the copper surfaces during their exposure to acidic sulphate solutions containing the inhibitors under investigation. Figure 7 presented the AFM image of a freshly electropolished Cu(111) surface immersed in the inhibitor-free base solution. As a result of the metal pretreatment procedures employed, the surface of the metal presented a high surface roughness, which was expressed in terms of the RMS parameter.

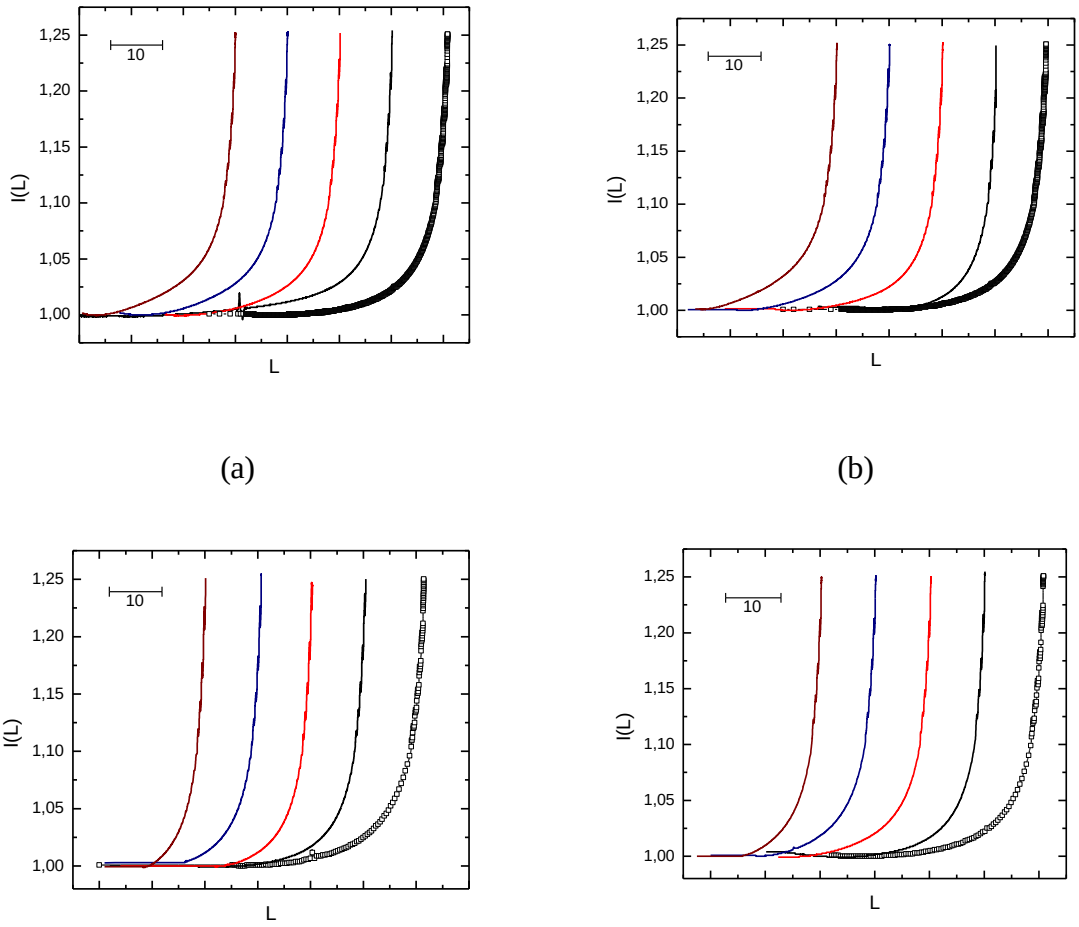


**Figure 5: SECM Approach plots after: (—) 3 min, (—) 1 hr, (—) 2 hrs, and (—) 3 hrs of exposure to 0.1 M $Na_2SO_4$ solution with (–□–) and without inhibitors: (a) 5-BDT, (b) 5-IPBDT, (c) 5-MBDT, and (d) 5-TDT. Inh. Conc.: 5x$10^{-5}$ M., Tip potential: +0.5 V vs SCE**

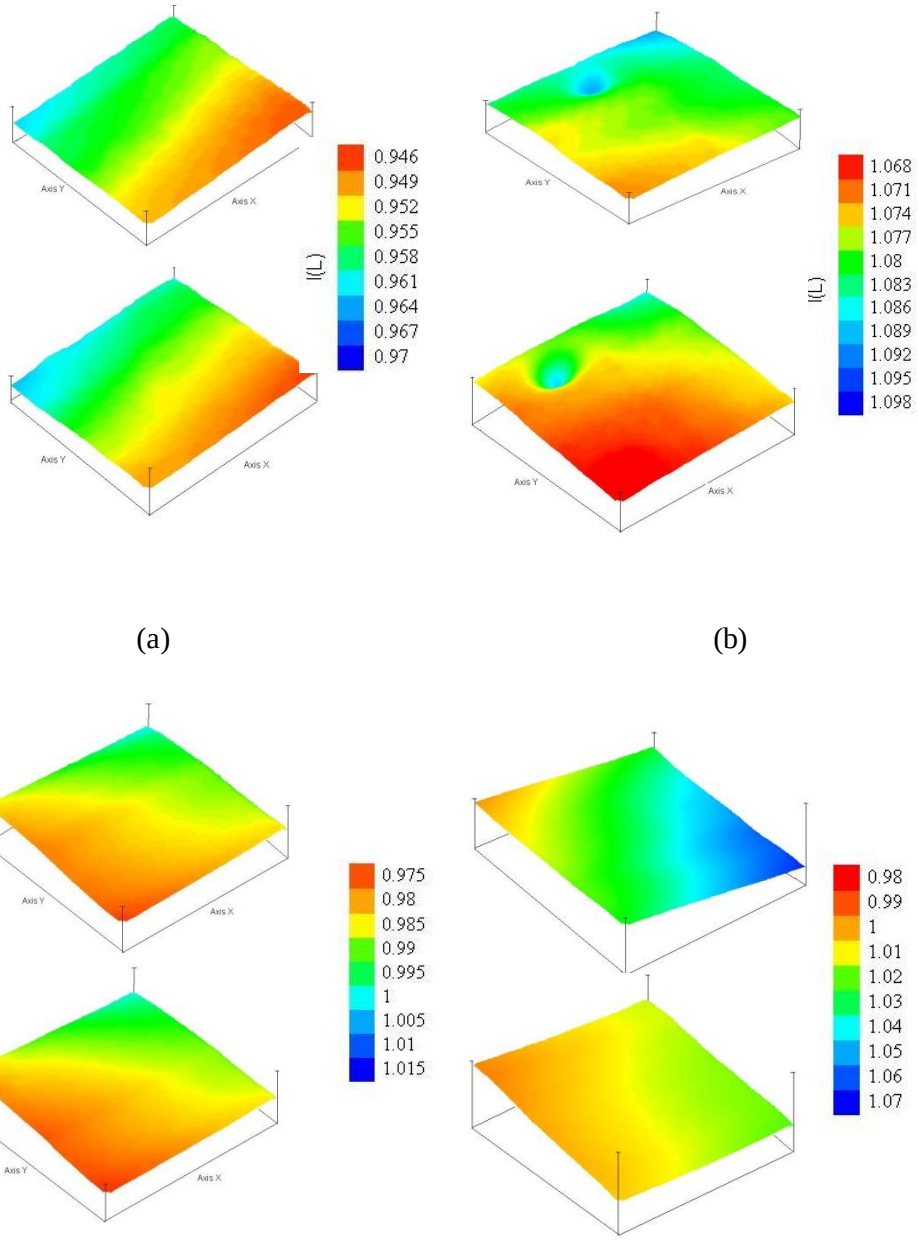


(a) (b)

(c) (d)

**Figure 6: SECM images of copper surfaces in acidic 0.1 M $Na_2SO_4$ + 1mM ferrocene-methanol solution after (up) 3 min, (down) 3 hrs exposure; then in $5x10^{-5}$ M of the inhibitors: (a) 5-BDT, (b) 5-IPBDT, (c) 5-MBDT, and (d) 5-TDT. Tip potential: +0.5 V**

**vs. Ag/AgCl/KCl (saturated) reference electrode. The images represent an area of 200 µm x 200 µm in X and Y directions.**

Changes induced in the surface of the copper samples by the presence of the thiazoles in the electrolyte can be observed from the AFM images given in fig. 8. The addition of the inhibitors produced a significant smoothing of the surface of the samples compared to that in the blank solution (fig. 7). This observation is evidence that the copper substrate was covered by an inhibitor layer in this case. Among the tested inhibitors, 5-IPBDT produced the smoothest surface and therefore the most effective protection of the copper.

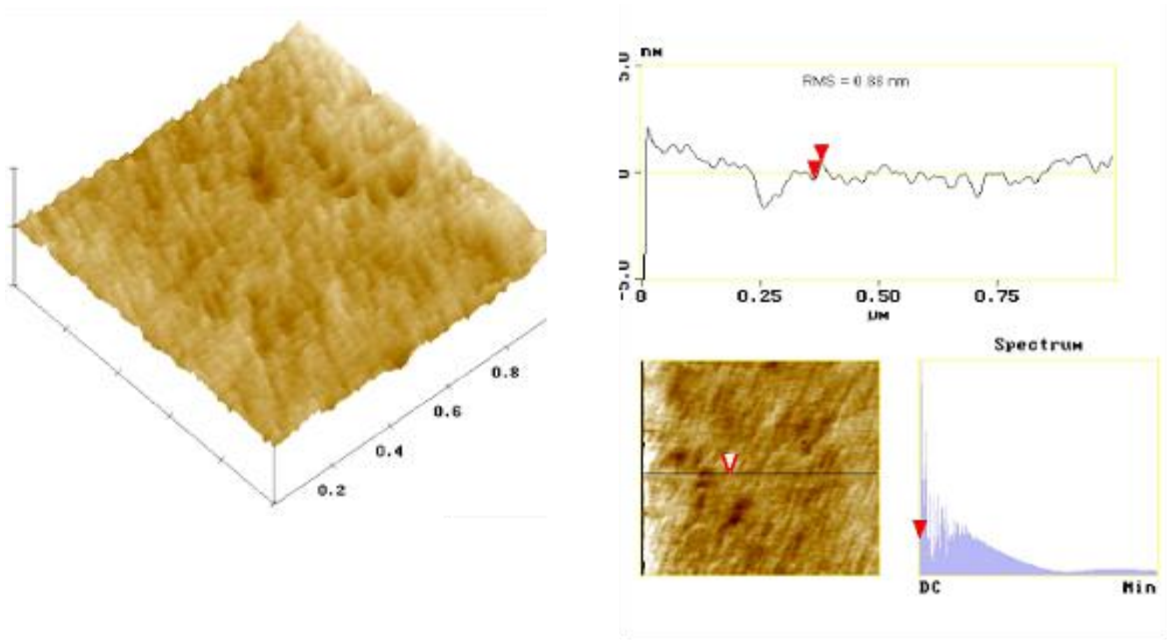


**Figure 7. AFM image of freshly electropolished Cu(111) single crystal immersed in 0.1 M $Na_2SO_4$ solution acidified at pH = 2.94.**

The protective effect of 5-IPBDT was investigated with more detail by using STM imaging. Figure 9 shows the surface morphologies of the electropolished Cu (111) surface exposed to the acidic sulphate containing solution and of the same surface shortly after changing the electrolyte to 5-IPBDT-containing solution. The STM image provided some evidence that the addition of 5-IPBDT to the electrolyte promoted some reorganization of the copper surface.

In fact, the presence of the inhibitor masked the atomic terraces and smoothed the surface, while the local imperfections were still visible.

The atomic terraces were still visible on some sites, which indicated that the surface was only partially covered with 5-IPBDT. However, the surface morphology did not change significantly during the measurement; only the stepped structure became less visible which could be explained by the 5-IPBDT molecule reordering on the copper surface.

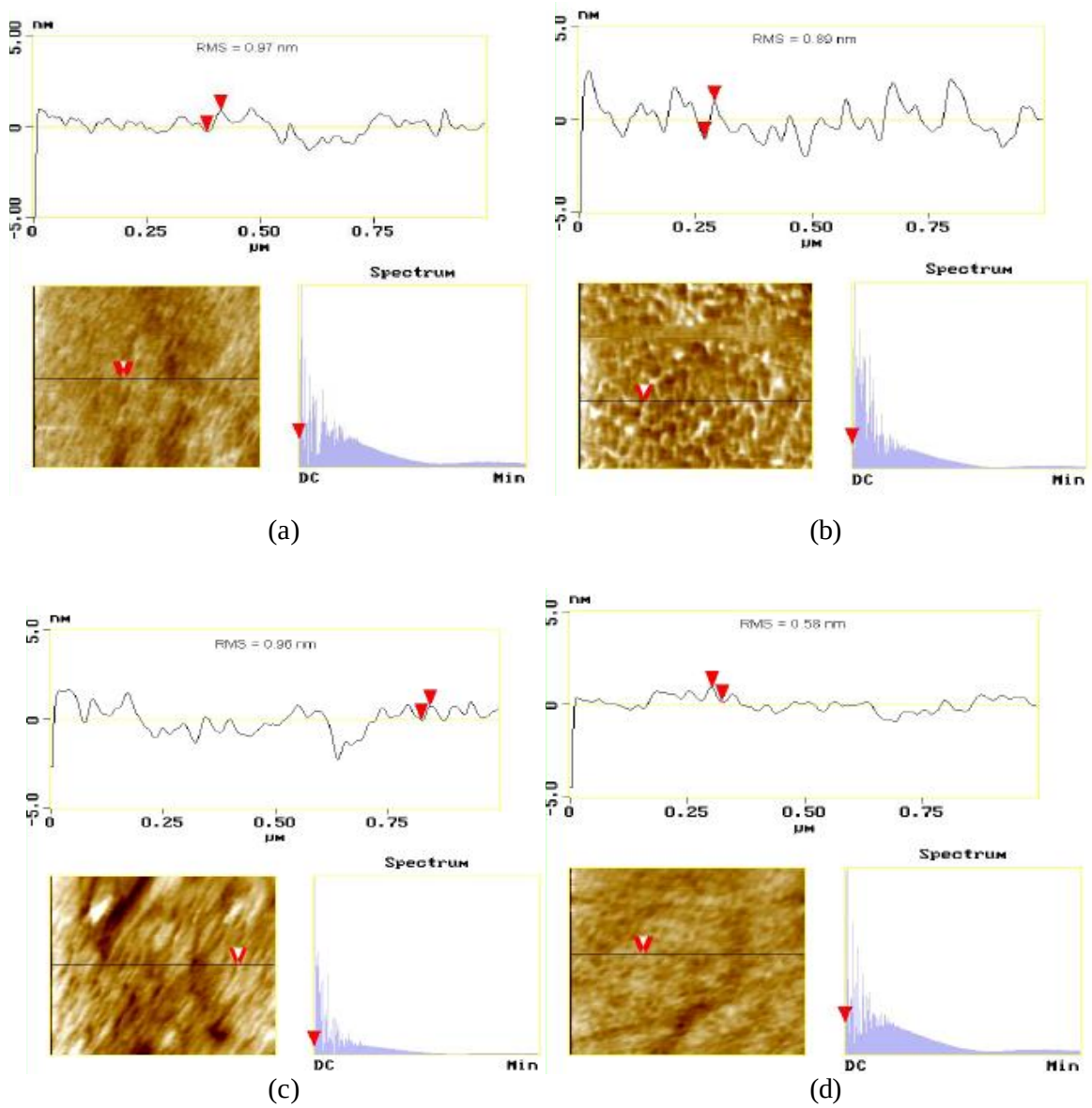


**Figure 8. AFM images of electropolished Cu(111) single crystal immersed in 0.1 M $Na_2SO_4$ solution with the addition of: (a) 5-IPBDT, (b) 5-BDT, (c) 5-TDT, or (d) 5-MBDT.**

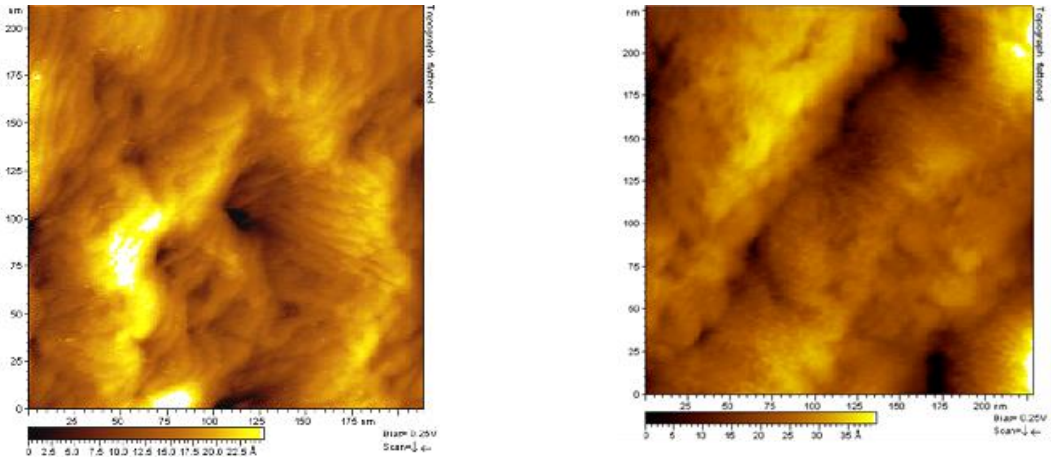

**Figure 9: STM images of Cu (111) surface in solution: (left) in acidic solution containing 0.1 M Na2SO4, and (right) shortly after the addition of the test solution containing 5-IPBDT.**

## 4. Conclusion

- A micro- and nano- electrochemical approach is necessary for the investigation of the role of adsorption-type inhibitors for metal corrosion.
- Thiazole derivatives are promising compounds for the inhibition of copper corrosion in acidic environments due to their capacity to adsorb on the metal surface through the nitrogen and sulphur atoms present in the structure of the molecules, whereas the longer chain may serve as a protecting shield on the copper electrode surface.
- The QCm results indicated that addition of thiazole derivatives to the electrolyte significantly decreased the dissolution rate of copper. The protection efficiency provided by these inhibitors followed the sequence: 5-IPBDT > 5-BDT > 5-TDT > 5-MBDT.
- The combined observations of only one relaxation time constant in the electrochemical impedance spectra, and the absence of changes in the conductivity of the surface with time as seen from the approach curves taken with the scanning electrochemical microscope, are evidences that these inhibitors adsorbed as a 2D

type. The thickness of these layers did not grow in size and were in the order of a mono or even partial monolayer.

- Surface imaging at the nanoscopic level led to the finding that the addition of the inhibitors produced a significant smoothing of the surface of the samples, which was evidence that the copper substrate could be covered by inhibitor layers in the acidic sulphate environment.

**Acknowledgement**

This work was supported by AKI and by the Ministry of Education, Science and Technological Development of the Republic of Serbia (Project No. 172013).

**References**

1. G. Trabanelli, *Corrosion, Mechanism*, F. Mansfeld (Ed), Marcel Dekker, New York, (1987) p. 119
2. G. Schmitt, *Brit. Corros. J*. **19** (1984) 165
3. V. Ashworth, D. Fairhust, *J. Electrochem. Soc.* **124** (1977) 506
4. J. van Muylder, *Comprehensive Treatise of Electrochemistry*, J.O'M. Bockris, B.E. Conway, E. Yeager, R.E. White Ed(s)., Plenum Press, New York, 1981, p.1
5. M.R.G. de Chialvo, R.C. Salvarezza and A.J. Arvia, *J. Appl. Electrochem.* **14** (1984) 165
6. Yu. I. Kuznetsov, M. O. Agafonkina, H. S. Shikhaliev, N. P. Andreeva and A. Yu. Potapov, *Int. J. Corros. Scale Inhib*. **3** (2) (2014) 137
7. M. Antonijevic, M. Petrovic, *Int. J. Electrochem. Sci*. **3** (2008) 1
8. S. Abuthahir, K. J. Vigrant, R. Vignesh, C. Vignseh, J. Abdul Nasser, Vijaya and S. Rajendran, *Journal of Chemical and Pharmaceutical Research*, 2015, 7(10S):193-200
9. M.R.G. de Chialvo, J.E. Zerbino, S.L. Marchiano, A.J. Arvia, *J. Appl. Electrochem.* **16** (4) (1986) 517
10. M.G. Figueroa, R.C. Salvarezza, A.J. Arvia, *Electrochim. Acta* **31** (6) (1986) 671
11. A. K. Satpati, A. V. R. Reddy, *International Journal of Electrochemistry* **2011** (2011) ID 173462
12. J. Gómez Becerra, R.C. Salvarezza, A.J. Arvia, *Electrochim. Acta* **33** (1988) 613.
13. M. Pérez Sánchez, M. Barrera, S. González, R.M. Souto, R.C. Salvarezza, A.J. Arvia, *Electrochim. Acta* **35** (1990) 1337

14. M.M. Laz, R.M. Souto, S. González, R.C. Salvarezza, A.J. Arvia, *Electrochim. Acta* **37** (1992) 655
15. R.M. Souto, M. Pérez Sánchez, M. Barrera, S. González, R.C. Salvarezza, A.J. Arvia, *Electrochim. Acta* **37** (1992) 1437
16. R.M. Souto, M. Pérez Sánchez, M. Barrera, S. González, R.C. Salvarezza, A.J. Arvia, *Electrochim. Acta* **38** (1993) 703
17. R.M. Souto, S. González, R.C. Salvarezza, A.J. Arvia, *Electrochim. Acta* **39** (1994) 2619
18. RM. Souto, M.M. Laz, S. González, *Anales de Química*, *International Edition* **93** (1997) 252
19. S. González, M. Pérez, M. Barrera, A.R. González Elipe, R.M. Souto, *J. Phys. Chem. B* **102** (1998) 5483
20. F. Mansfeld (Ed.), *Corrosion Mechanisms*, Marcel Dekker, New York, (1987) p. 119
21. G. Trabanelli. *Corrosion* **47** (1991) 410.
22. L. Kiss, *Kinetics of Electrochemical Metal Dissolu*tion, Elsevier, Amsterdam, (1988) p. 278-287
23. A. Shaban, E. Kálmán, J. Telegdi, *Electrochim. Acta* **43** (1998) 159
24. A. Jardy, A. Legal Lasalle-Molin, M. Keddam and H. Takenouti, *Electrochim. Acta* **37** (1993) 2195
25. E. Stupnisek-Lisac, A. Gazioda, M. Madzarac, *Electrochim. Acta* **47** (2002) 4189
26. Y. Tan, M. Srinivasan, S. Pehkonen, S. Chooi, *Corros. Sci*. **48** (2006) 840
27. M. Antonijevic, S. Milic, S. Šerbula, G. Bogdanovic, *Electrochim. Acta* **50** (2005) 3693
28. A.C.C. Mary, S. Rajendran, R.J. Rathish, A. Krishnaveni - *Int. J. Nano. Corr. Sci. Engg*, 2 (3) (2015) 46-59
29. M. Itoh, H. Nishihara, K. Aramaki, *J. Electrochem. Soc*. **142** (1995) 1839
30. M. B. Petrović Mihajlović, M. M. Antonijević, *Int. J. Electrochem. Sci*. **10** (2015) 1027
31. A. Shaban, Gy. Vastag, A. Pilbáth, I. Kék, L. Nyikos, *J. Mater. Environ. Sci*. **7** (7) (2016) 2572
32. N. Ohno, J. Uehara, K. Aramaki, *J. Electrochem. Soc*. **140** (1993) 2512
33. J. Nakomčić, Gy. Vastag, A. Shaban, L. Nyikos, *Int. J. Electrochem. Sci*. **10** (2015) 5365
34. Gy. Vastag, J. Nakomčić, A. Shaban, *Int. J. Electrochem. Sci*. **11** (2016) 8229
35. Y.I. Kuznetzov, *Organic Inhibitors of Corrosion of Metals*, A.D. Mercer and J.G.N. Thomas Ed(s)., Plenum Press, New York, 1996, p.101
36. F. Ammelot, C. Faiud, E.M.M. Sutter, *Electrochim. Acta* **42** (1997) 3565
37. C.W. Yan, H.C. Lin, C.N. Cao, *Electrochim. Acta* **45** (2000) 2815

38. M. Fonsati, F. Zucchi, G. Trabanelli, *Electrochim. Acta* **44** (1998) 311
39. H. Otmacic, E. Stupnisek-Lisac, *Electrochim. Acta* **48** (2003) 985
40. N. Huynth, T. Notoya, S.E. Bottle, D.P. Schweinsberg, *Corros. Sci*. **42** (2000) 259
41. F. Zucchi, G. Trabanelli, M. Fonsati, *Corros. Sci*. **38 (**1996) 2029
42. M. Fonsati, F. Zucchi, G. Trabanelli, *Electrochim. Acta* **44** (1998) 311
43. M.-K. Hsieh, D. A. Dzombak, R. D. Vidic, *Ind. Eng. Chem. Res*. **49** (16) (2010) 7313
44. Gy. Vastag, E. Szőcs, A.Shaban, E. Kálmán, *Pure Appl. Chem*. **73** (2001) 1861
45. C. Wang, S. Chen, H. Ma, L. Hua, N. Wang *J. Serb. Chem. Soc*. **67** (2002) 685
46. E. Abelev, D. Starosvetsky, Y. Ein-Eli, *Langmuir* **23** (2007), 11281
47. E. M. Sherif, R. M. Erasmus, J. D. Comins, *J. Colloid Interf. Sci*. **309** 2 (2007) 470
48. H. O. Curkovic, E. Stupnisek-Lisac, H. Takenouti, *Corros. Sci*. **52** 2 (2010) 398
49. E. M. Sherif, R. M. Erasmus and J. D. Comins, *J. Colloid Interf. Sci*. **311** 1 (2007) 144
50. M. A. Amin, *J. Appl. Electrochem*. **36** (2) (2006) 215
51. M. Scendo, *Corros. Sci*. **49** (2007) 2985
52. E. Szőcs, G. Vastag., A. Shaban, E. Kálmán, *Corros. Sci*. **47** (4) (2005) 893
53. B.J. Cruickshank, A.A. Gewirth, R.M. Rynders, R. Alkire, *J. Electrochem. Soc.* **139** (1992) 2829
54. M.R. Vogt, W. Polewska, O.M. Magnussen, R.J. Behm, *J. Electrochem. Soc.* **144** (1997) L113
55. O.M. Magnussen, M.R. Vogt, J. Scherer, R.J. Behm, *Appl. Phys. A*, **66** (1) (1998) S447
56. M.R. Vogt, A. Lachenwitzer, O.M. Magnussen, R.J. Behm, *Surf. Sci*. **399** (1) (1998) 49
57. W. Polewska, M.R. Vogt, O.M. Magnussen, R.J. Behm, *J. Phys. Chem. B* **103** (1999) 10440
58. O.M. Magnussen, R.J. Behm, *Mater. Res. Bull.* **24** (1999) 16.
59. A. Shaban, Gy. Vastag, L. Nyikos, *Int. J. Corros. Scale Inhib*. **4** (4) (2015) 328
60. Gy. Vastag, E. Szőcs, A. Shaban, I. Bertóti, K. Popov-Pergal, E. Kálmán, *Solid State Ionics* **141–142** (2001) 87
61. K. Mansikkamäki, P. Ahonen, L. Murtomäki, G. Fabricius, K. Kontturi, *J. Electrochem. Soc*. **152** (2005) B12
62. K. Mansikkamäki, U. Haapanen, C. Johans, K. Kontturi, M. Valden, *J. Electrochem. Soc.* **153** (2006) B318
63. G. Sauerbrey, *Zeitschrift für Physik* **155** (1959) 206
64. S. Bruckenstein, M. Shay, *Electrochim. Acta* **30** (1985) 1295.

RECEIVED:2-2-17
Accepted:8-3-17